SHOCK PAIR OBSERVATION

J. K. Chao, V. Formisano and P. C. Hedgecock

ABSTRACT

On day 84, 1969, the HEOS 1 satellite observed a shock pair connected with a plasma bulk velocity increase from 400 to ~ 750 km/sec. Both shocks were fast shocks. The forward shock had a Mach number of 1.7, the reverse shock had $M_{fast} = 1.4$. The time interval between the two shocks was 7 hr, 10 min. The time delay between HEOS 1 and Explorer 35 reverse shock observation (20 ± 6 min) agrees with the computed time delay (11 ± 4 min).

INTRODUCTION

The HEOS 1 satellite was launched December 5, 1968, and provided good plasma and magnetic data for almost 2 years. Because of its elongated orbit, it was able to observe the solar wind for a high percentage of time. Plasma and magnetic data concerning a shock pair observation are shown in this paper.

The shock pairs have been theoretically studied by *Sonett and Colburn* [1965] and *Hundhausen and Gentry* [1969]. Experimentally they have been studied indirectly from sudden impulses observed in the ground station magnetograms by *Razdan et al.* [1965], but to our knowledge no direct observation has been published. The forward shocks have been observed more frequently in the solar wind. A reverse shock was recently reported by *Burlaga* [1970].

Instrument details and data analysis are reported by *Bonetti et al.* [1969] and *Hedgecock* [1970].

PLASMA OBSERVATIONS

Plasma observations are shown in figure 1, which gives plasma bulk velocity V_p; proton number density N_p; proton most probable thermal speed W_p; the value of the index K assumed for the distribution used to fit the data and total energy density, proton thermal energy density, electron thermal energy density (assumed to be three times greater than that of protons), and magnetic energy density. Periods when α particles were observed are indicated with a thick line.

$$F_K(W) = \frac{K!}{K^{3/2}\,[K-(3/2)!]\,\pi^{3/2}\,W_O^{\,3}} \; \frac{1}{[1+(W^2/KW_O^{\,2})]^{K+1}} \qquad (1)$$

The bulk speed shows an increase over 10 hr from 400 km/sec to almost 750 km/sec. This increase starts gradually from 0400 UT (400 km/sec) to 0645 (450 km/sec) then shows a complicated discontinuous structure. As we shall see later two fast shocks are present in this structure: one observed at 0645 UT and another at 1355 UT. Plasma parameters for the discontinuities are given in table 1.

The proton number density shows a large increase before the high speed plasma, at the beginning of the velocity gradient. The thermal speed reaches very high values when the bulk speed gradient is observed. Correspondingly, the total energy density, very steady before the first shock, becomes very large and very fluctuating within the velocity gradient. It should be remembered, however, that the "ad hoc" hypothesis that electron thermal energy density is three times proton thermal energy density will enhance the fluctuations due to tangential discontinuities rather than cancel them, as it should if the total pressure is balanced.

Drs. Chao and Formisano are at the Laboratorio Plasma Spaziale, University of Roma, Rome; Dr. Hedgecock is at the Imperial College of Science and Technology, London.

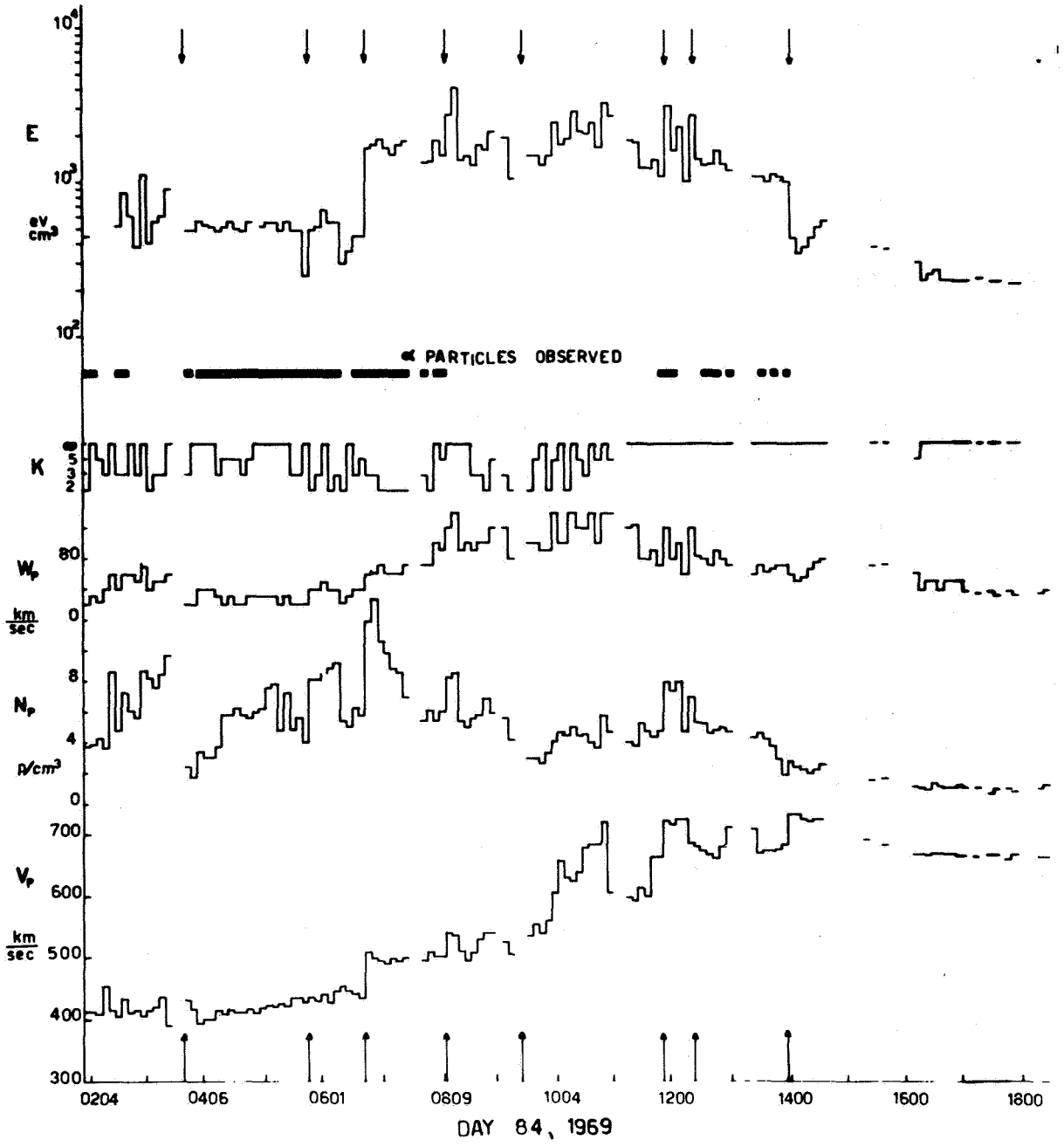

Figure 1. *Plasma time history during the shock pair period, day 84, 1969. From the bottom are given plasma bulk velocity (note the very compressed scale) proton number density N_p, most probable thermal speed and total energy density (see text). Periods of α particles observations are indicated. Arrows indicate eight discontinuities discussed in the text.*

The distribution function is constantly maxwellian ($K = \infty$) when high speed plasma is observed, while it shows a long high energy tail ($K = 2$) just after the first shock.

Alpha particles were observed during few short periods of time. Figure 2 shows the α particle bulk velocity V_α, number density N_α, and most probable thermal speed W_α time history during the first shock crossing. As has

Table 1. *Data from HEOS 1*

Time	B_1	B_2	V_1	V_2	N_1	N_2	W_1	W_2	θ_{B1}	ϕ_{B1}	θ_{B2}	ϕ_{B1}	ϕ_{V1}	ϕ_{V2}	$T_e \times 10^5$		
0339	9.6	14.0	390	430	9.8	2.4	60	20	30°	60°	20°	60°			1.5	2.3	D
0548	13.0	10.0	425	430	3.8	8.0	20	40	5°	60°	− 5°	75°			1.5	2.0	D
0645	10.0	18.0	430	510	6.0	12.5	40	60	−35°	80°	−35°	80°	−4.5°	−6.1°	1.5	Negative	Sf
0811	20.0	14.5	500	530	5.8	8.2	90	120	−20°	85°	−70°	90°			1.5	1.6	
0930	13.5	19.0	505	535	4.1	2.9	80	100	50°	130°	80°	230°			1.5	Negative	
1155	18.0	12.0	660	720	4.7	7.9	70	120	70°	170°	20°	200°			1.5	Negative	
1230	15.3	19.6	685	670	6.9	5.2	120	80	−10°	180°	38°	205°			1.5	1.6	D
1355	17.5	9.5	710	750	$1.9/\overline{4.0}$ (*)	$2.6/\overline{2.5}$ (*)	70	60	20°	210°	20°	185°	−1.3°	−18.8°	1.5	21	Sr

D discontinuity (total pressure is balanced).
S shocks (total pressure not balanced; Sf, forward shock; Sr, reverse shock).
(*) single value and average value (−) are given.

been already pointed out in general by *Formisano et al.* [1970*a*], in this case the behavior of the α particles is not simple. No relevant velocity change is observed for V_α when the shock is observed, while a large discontinuity is observed 12 min before the shock: V_α goes from 432 km/sec (0615 UT) to 515 km/sec (0632 UT) (two measurements are missed in between). This abrupt increase of V_α, however, is observed together with a decrease of N_α, if we compare the N_α value observed two measurements before; since the data gap is partially due to low α particles fluxes, an increase of N_α together with the increase of velocity V_α cannot be excluded. An increase of N_α is observed for a short period in coincidence with the proton shock.

No electron measurements were available. However, assuming for charge neutrality $N_e \simeq N_p$ and $T_e = 1.5 \times 10^5$ °K on one side of the considered discontinuities, the electron temperature was computed on the other side in order to balance the pressure on both sides of the discontinuities [*Burlaga and Chao*, 1971]. As shown in table 1, four out of eight cases gave a very reasonable electron temperature on side two; these were called *tangential discontinuities.* In three cases, the electron temperature became negative, meaning that the pressure on side two was already much higher than on side one. The 0645 UT event will be shown later, as a forward shock. The last discontinuity needed an increase of the electron temperature of a factor of 20 on side two for the total pressure being balanced. The expected side two electron temperature is therefore very unlikely. This discontinuity will be shown later as a reverse shock.

We are left with two discontinuities observed at 0930 UT and 1155 UT for which it is difficult to balance the pressure. As we will see later from the magnetic field, both of them have a very different character as observed by HEOS 1 and Explorer 35. Therefore, we may tentatively conclude that these are two discontinuities in a nonsteady state. However, wave energy should also be taken into account in balancing the energy density across the discontinuities.

MAGNETIC FIELD OBSERVATIONS

HEOS 1 magnetic field observations are shown in figure 3. The satellite had just crossed the laminar structure of earth-bow shock studied by *Formisano et al.* [1970b]. The spikes observed in the magnetic field intensity at 0220 UT and 0357 UT are very short magnetosheath observations due to the fast moving bow shock.

The magnetic field intensity shows a very clear structure that can be described as follows:

1. *The preceding "square wave."* From 0339 UT to 0548 UT magnetic field intensity is very large (14γ) and very steady. A sharp tangential discontinuity is observed at 0425 UT; θ changes from +20° to 30° while B remains constant. It is not clear whether this structure is related to the proton bulk velocity gradient and the shock pair.

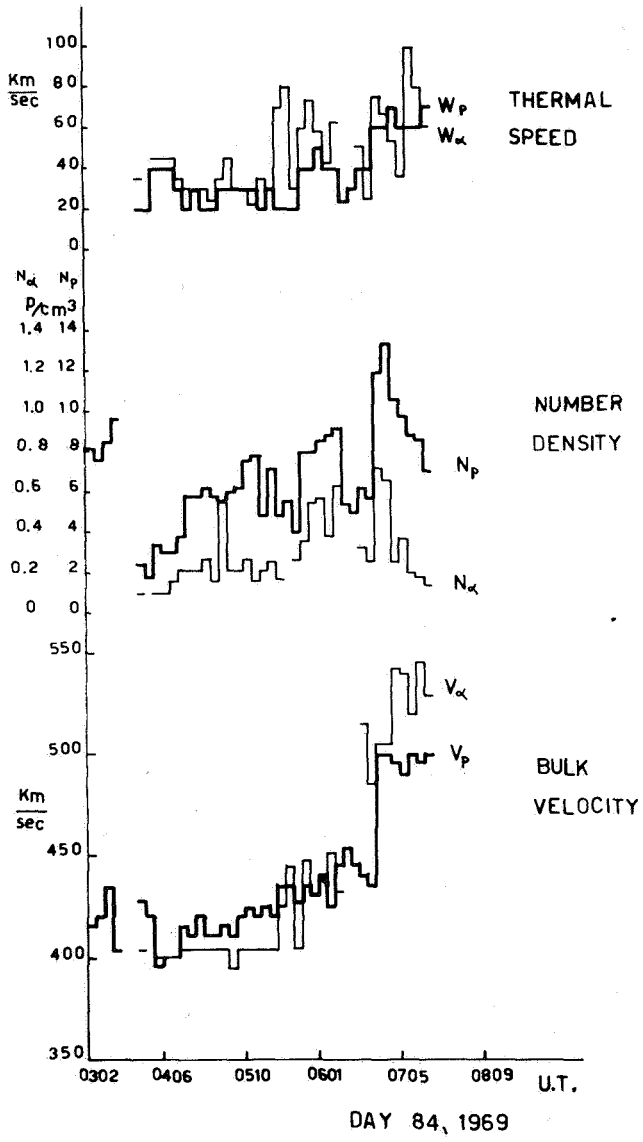

Figure 2. *Alpha particles and proton parameters across the forward shock. Thick lines are for protons, thin for α particles. Note that two measurements give high speed α particles before the proton shock.*

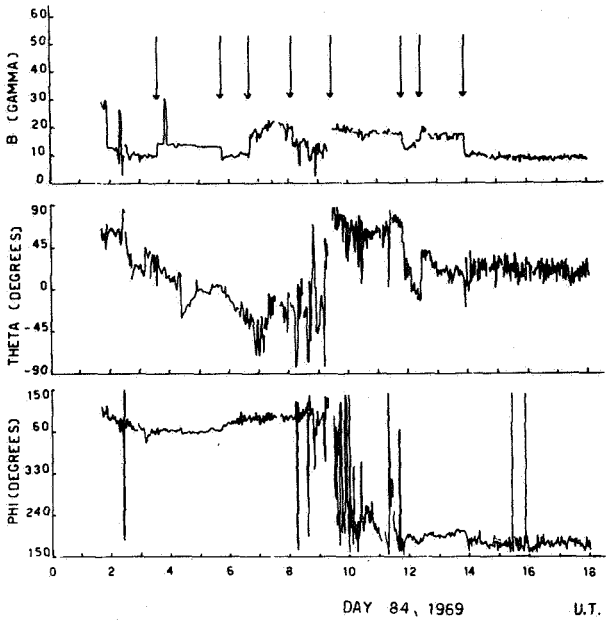

Figure 3. *HEOS 1 magnetic field during the shock pair period, day 84, 1969. The satellite just left the bow shock at 0158 UT. (Two short magnetosheath periods are shown later by the magnetic field intensity as spikes.) Arrows indicate the eight discontinuities discussed in the text.*

2. *The shock pair.* Magnetic field intensity shows the forward shock at 0645 UT when the field magnitude abruptly changes from 10γ to 18γ. After the shock, B increases until it reaches 22γ; later at 0811 UT, B decreases suddenly to 14.5γ. From 0811 to 0930 UT both magnetic field intensity and direction are very turbulent and show large fluctuations. From 0930 to 1155 UT only the magnetic field direction shows large fluctuations. A second depression of magnetic field intensity of ~5γ is observed between 1155 and 1230 UT. The reverse shock finally reaches the satellite at 1355 UT.

Figure 4 shows the magnetic field observed by Explorer 35. The position of the satellite is shown in figure 5; it was around the moon at ~79° from the earth-sun line on the evening side.

Explorer 35 magnetic field observations show the same general configuration as for HEOS 1. However, a few important differences should be noted:

1. The reverse shock is observed at UT 1415, 20 min later than the HEOS 1 observation.
2. The second "depression" of the magnetic field intensity, clearly identified by the changes of the direction, is observed between UT 1234 and 1303:39÷33 min later than HEOS 1. The amplitude of this magnetic field intensity depression is now 2÷2.5γ instead of 5γ.
3. A data gap between 0606 and 0652 UT does not allow a comparison between time observation of the two satellites for the forward shock.
4. The first "depression" of the magnetic field intensity is only partially observed because of a data gap; the observed part looks different for the HEOS 1 observations.

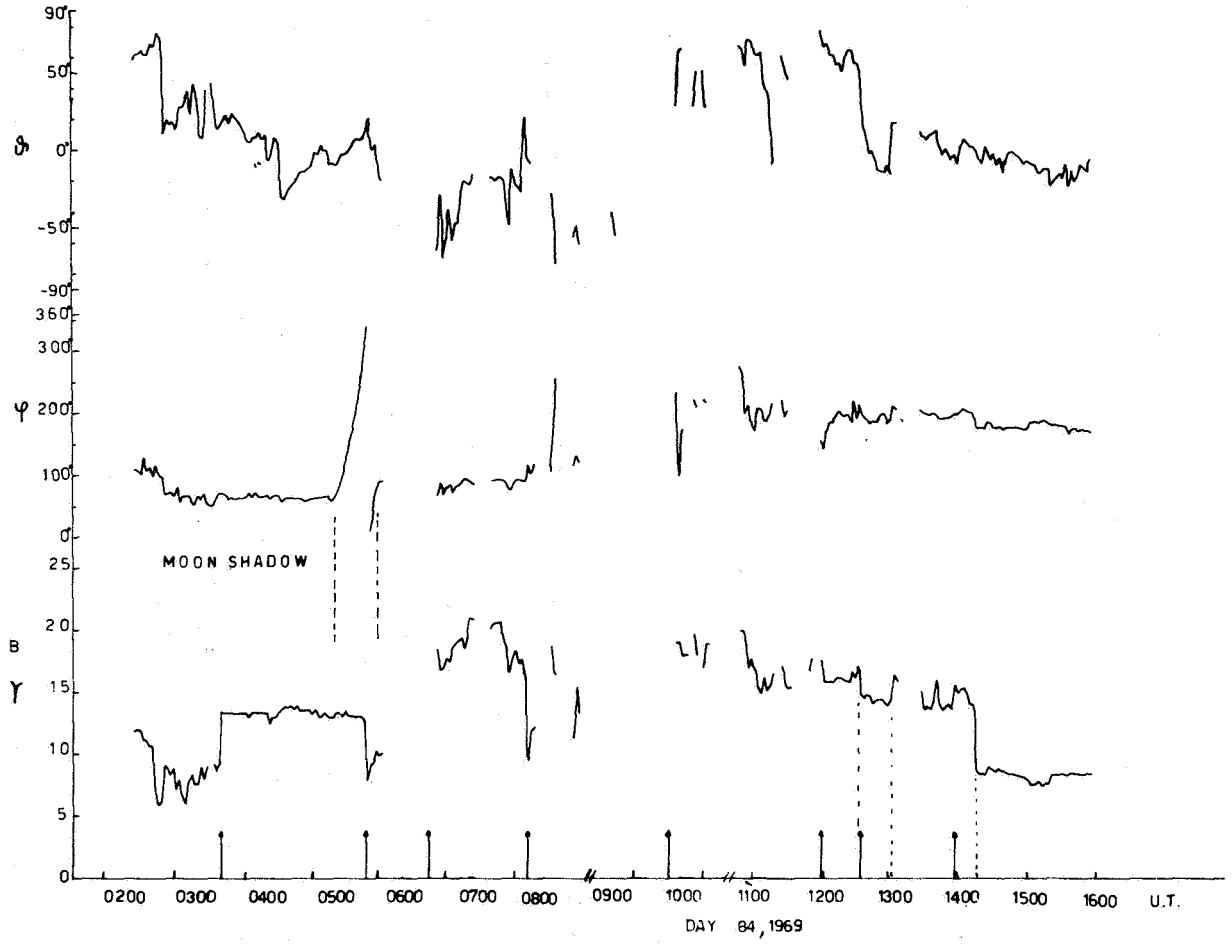

Figure 4. *Explorer 35 magnetic field during the shock pair observation, day 84, 1969. Arrows indicate the eight discontinuities discussed in the text at the observation time of HEOS 1. Between 0500 and 0600 UT the magnetic field direction is altered by the moon's shadow.*

THE FORWARD SHOCK

The procedure described by *Chao* [1970] was used to obtain a set of 14 parameters (see table 2) (B_{R1}, B_{T1}, B_{N1}, B_{R2}, B_{T2}, B_{N2}, V_{R1} V_{T1}, N_{N1}, V_{R2}, V_{T2}, V_{N2}, n_1, n_2); these satisfy the Rankine-Hugoniot equations for an isotropic plasma and are close to the observed average values on both sides of the discontinuity (table 2). We will call this set of parameters the *computed parameters* associated with the discontinuity. When these computed parameters are within the uncertainty of the corresponding average values, we have shown that the present event is a shock.

In table 2 we use the RTN coordinates in which the R axis is out from the sun and parallel to the sun-earth line, the T axis is the direction of the motion of the earth, the R-T plane is parallel to the ecliptic, and the N axis is northward and perpendicular to the ecliptic. The polar coordinates are also used in table 2. The "computed parameters" and the measured average values are given. The close agreement shows that the observed parameters and changes are consistent with the Rankine-Hugoniot equations.

In principle, using the Rankine-Hugoniot equations, it is possible to solve for 1 of the 12 known parameters as a function of the remaining 11 [*Chao and Olbert*, 1970].

It should be noted that the N component of the solar wind bulk velocity was not available, therefore we assume that V_{N2} is zero. We can solve for V_1 as a function of (B_1, B_2, V_3, n_1,n_2). Then, the measured parameters B_1, B_2, V_2, n_1, n_2 are allowed to vary independently within their uncertainties for computing the V_1 value. When the computed value of V_1 is within the uncertainties of its measured average value,

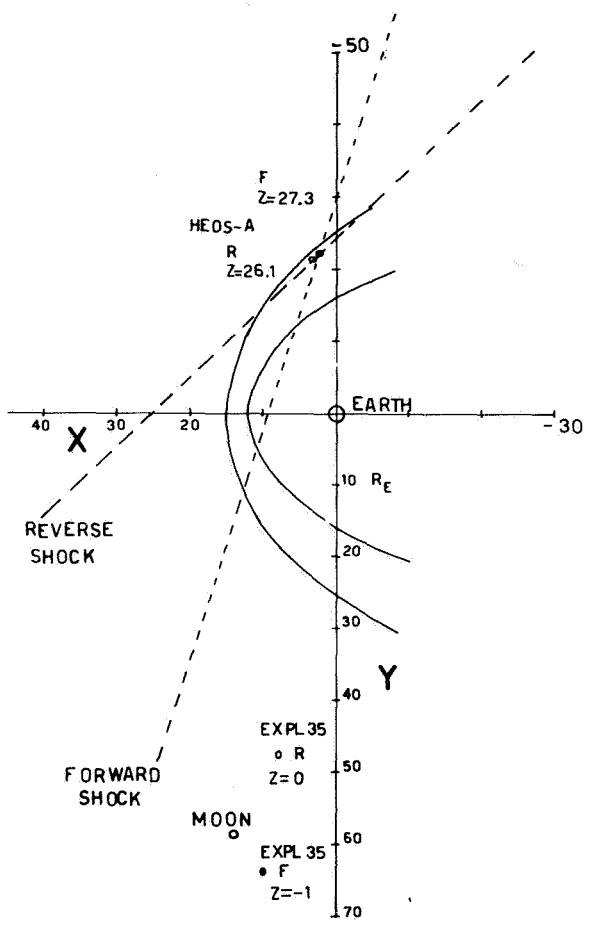

Figure 5. *HEOS A and Explorer 35 relative positions at the forward (F) and reverse (R) shock observation. The X-Y plane is the plane of the ecliptic, the Z component is also given each time. Dashed lines are the intersections of the two-plane assumed shock surfaces with a plane parallel to the ecliptic plane.*

then this computed value can be regarded as a prediction. Table 2 shows that the predicted and observed values of V_1 are in good agreement.

It should be noted that the solution gives a reasonable component of solar wind bulk velocity perpendicular to the ecliptic plane, unknown from the data. This shock is a perpendicular shock for the following reasons:

1. The magnetic field does not change in direction across the discontinuity but change in strength by a factor of 1.9 ± 0.1.
2. The ratio of number densities across the perpendicular shock equals the ratio of magnetic field strength (i.e., $B_1/B_2 = N_1/N_2$) as it should.

The shock velocity in an RTN frame of reference is given in table 3 together with other basic shock parameters. In this table, V_s is the shock velocity in RTN coordinate, $\hat{n}$ is the shock normal in RTN and solar ecliptic coordinates θ, ϕ, and V_n^* is the normal component of the flow to the shock front expressed in the shock frame of reference; $\theta_{B,n}$ is the angle between B and $\hat{n}$; M_A is the Mach number based on the *total* magnetic field intensity and $\hat{n} \cdot M_{fast}$ is the Mach number based on the fast mode magnetosonic wave propagating along the shock normal. The fast Mach number is 1.7; that is, it fulfills the necessary condition for a shock pair to develop ($M > 1.5$) found by *Hundhausen and Gentry* [1969].

From the shock normal and shock speed the time delay between HEOS 1 and Explorer 35 observations was computed.

The Explorer 35 shock distance was $14.4\, R_e \pm R_e$ and the time delay predicted is 2.6 min. The time delay observed, because of data gap, has to be $-39 < \tau > 7$ min; therefore there is no inconsistency.

Figure 5 shows the intersection of the shock surface with a plane parallel to the ecliptic and passing through the HEOS 1 position.

THE REVERSE SHOCK

The best-fit procedure also has been used for the reverse shock, with very good agreement obtained between predicted and observed parameters (table 4). The shock Mach number was 1.4. The shock was moving backward along its normal with a speed of 160 km/sec. The Alfvén Mach number was now computed using only the normal component of B to the shock surface.

From the shock normal and shock velocity the time delay between HEOS 1 and Explorer 35 observations has been computed. The Explorer 35 to shock distance was 40.8 R_e and the time delay predicted was 11 min. It should be remembered, however, that because of the geometry of the problem (fig. 5) an error as small as 7° for the shock normal would give 2 min of error on the time delay. Another ~2 min can be attributed to a 10 percent error on the shock velocity. The time delay is therefore 11 ± 4 min. The observed time delay is 20 ± 6 min.

From the basic shock parameters we see that in this case electron temperature almost does not change across the discontinuity. The forward and reverse shocks cannot be tangential discontinuities. If they were tangential discontinuities the predicted time delay between HEOS 1 and Explorer 35 disagrees with the measured delay time.

The best-fit method gives a possible value for the plasma anisotropy on both sides of the discontinuity: $\xi = 1 - (\beta_\parallel - \beta_\perp)/2$ is 0.0 in the preshock region and becomes 0.6 in the postshock region. This parameter had been assumed equal to 1 for the forward shock analysis.

Table 2. *Computed and averaged parameters for the forward shock*

Parameter	Computed values		Average values	
	Preshock	Postshock	Preshock	Postshock
B	-1.4, -8.1, -5.7	-2.3, -13.2, -13.4	-1.4, -8.1, -5.7	-2.3, -13.2, -13.4
(gamma)	10(-35°, 80°)	19(-35°, 80°)	10(-35°, 80°)	19(-35°, 80°)
V, km/sec	429, 0, -19	504, -25, 0	429, -6, 0	504, -25, 0
	430 (-2.5°, -0°)	510 (0°, 2.1°)	430 (0°, 0.5°) (*)	510 (0°, -2.7°) (*)
N, P/cm^3	6.00	11.0	6.0±20%	12.5±20%
W, km/sec	40	60	40±10 km/sec	60±10 km/sec

Explorer 35 to shock distance 14.4 R_e.
Explorer 35 to HEOS 1 time delay predicted 2.6 min.
Explorer 35 to HEOS 1 observed time delay $-31 < \tau < 7$ min.
(*) without aberration.

Table 3. *Basic shock parameters*

	Forward shock		Reverse shock	
$\mathbf{V}_s$, km/sec	548, -142, 130		251, -257, 71	
$\hat{n}$RTN (θ,ϕ)	0.929, -0.294, 0.224 13°, 162.4°		0.684, -0.703, 0.195 11°, 134.0°	
	Preshock	Postshock	Preshock	Postshock
$\mathbf{V}_n^*$	185	100	199	166
$\theta_{B,n}$	90°	90°	45°	66°
$\mathbf{M}_A$	2.07(*)	0.8(*)	6.4	2.1
M_{fast}	1.7	0.67	1.4	0.7
$T_e \times 10^5$ °K	2±1	3±1	2±1	1±1
ξ	1	1	0.0±0.2	0.6±0.2

(*) Using the intermagnetic field intensity.

Table 4. *Computed and averaged parameters for the reverse shock*

	Computed values		Average values	
	Preshock	Postshock	Preshock	Postshock
B	8.9, 0.0, 3.3	14.2, 5.8, +5.6		
(gamma)	9.5 (20°, 180°)	17.1 (20°, 202°)	9.5 (20°, 185°)	17.5 (20°, 210°)
V, km/sec	734, −123, 0	723, −9 2		
	745.0 (0°, −6.5°)	715 (0.1°, 0.7°)	750 (0°, −6.5°) (*)	710 (0°, +1°) (*)
N, P/cm^3	2.3	4.0	2.5±20%	4.0±20%
W, km/sec	60	70	60±10 km/sec	70±10 km/sec

Explorer 35 to shock distance 40.8 R_e ±7.5 R_e.
HEOS 1 to Explorer 35 predicted time delay 11 min ±4.
HEOS 1 to Explorer 35 observed time delay 20 min ±6.
(*) without aberration.

DISCUSSION

A shock pair observed by HEOS 1 and Explorer 35 has been studied. This shock pair also produces the classical SI^+ and SI^- pair in the H component of the geomagnetic field reported by most equatorial ground stations.

The shock analysis described by *Chao* [1970] has given a Mach number of 1.7 for the forward shock and 1.4 for the reverse shock. It seems therefore verified the necessary condition suggested by *Hundhausen and Gentry* [1969] for the forward shock Mach number ($M_p > 1.5$).

We suggest that the two magnetic field intensity "depressions" observed between 0811 and 0930 UT, 1155 and 1230 UT, be interpreted as decay of two discontinuities where the shocks were generated. Indeed the general structure of two shocks with two "depressions" in the magnetic field intensity has been verified on Pioneer 8 data. A statistical study made by some of the authors is in progress. With this assumption, and using the shock speeds relative to the ambient plasma (154 km/sec for the forward shock, 160 km/sec for the reverse shock) it is possible to compute the distance from the satellite where the shocks were generated.

The reverse shock has been observed by HEOS 1 1.5-2 hr after the assumed generation point. This time interval corresponds to a distance of 4.9 10^6 km using an average plasma velocity of 680 km/sec and has been covered by the shock with its velocity of 160 km/sec in 510 min, which corresponds to a *distance of 20.8 10^6 km* using the average plasma velocity.

For the forward shock, assuming as a generation point the discontinuity observed at 0930 UT, we obtain an age of 536 min corresponding to a *distance of 16.1 10^6 km,* using an average plasma speed of 500 km/sec.

The two shocks appear to be generated within the solar wind at a distance of 0.13 or 0.10 AU from the satellite toward the sun.

ACKNOWLEDGMENTS

We are very grateful to Drs. N. Ness and L. F. Burlaga of the Goddard Space Flight Center for providing unpublished magnetic data from Explorer 35. We thank also the S-58 Belgian experimenters and Prof. Coutrez who provided unpublished data for the solar wind direction and Dr. Signorini who helped in their analysis.

We are indebted, also, to the other people of the Laboratorio per il Plasma nello Spazio of Rome, who have participated in the development of the solar wind experiment.

This research has been supported by the Consiglio Nazionale delle Ricerche of Italy. The HEOS 1 magnetic field experiment was supported by the British Science Research Council.

REFERENCES

Bonetti A.; Moreno, G.; Cantarano, S.; Egidi, A.; Marconero, R.; Palutan, F.; and Pizzella, G.: Solar Wind Observations with the ESRO Satellite HEOS 1 in December 1968. *Nuovo Cimento B,* Vol. 64, 1969, p. 307.

Burlaga, L. F.; and Chao, J. K.: Reverse and Forward Slow Shocks in the Solar Wind. Preprint, 1971.

Burlaga, L. F.: A Reverse Hydromagnetic Shock in the Solar Wind. *Cosmic Electrodyn.,* Vol. 1, 1970, p. 233.

Chao, J. K.: Interplanetary Collisionless Shock Waves. MIT Center for Space Research Preprint CSR TR-70-3, 1970.

Chao, J. K.; and Olbert, S.: Observation of Row Shocks in Interplanetary Space. *J. Geophys. Res.,* Vol. 75, 1970, p. 6394.

Formisano, V.; Hedgecock, P. C.; Moreno, G.; Sear, J.; and Bollea, D.: Observations of Earth's Bow Shock for Low Mach Numbers. Preprint L.P.S.-70-13. Submitted to *Planet. Space Sci.* 1970*a*.

Formisano, V.; Moreno, G.; and Palmiotto, F.: α-Particles Observations in the Solar Wind. *Solar Phys.,* Vol. 15, 1970*b*, p. 479.

Hedgecock, P. C.: The Solar Particle Event of February 25, 1969, in *Intercorrelated Satellite Observations Related to Solar Events,* edited by V. Manno and D. E. Page. D. Reidel, Dordrecht-Holland, 1970, p. 419.

Hundhausen, A. J.; and Gentry, R. A.: Effects of Solar Flare Duration on a Double Shock Pair at 1 AU. *J. Geophys. Res.* Vol. 74, 1969, p. 6229.

Razdan, H.; Colburn, D. S.; and Sonett, C. P.: Recurrent SI^+–SI^- Impulse Pairs and Shock Structure in M–Region Beams. *Planet. Space Sci.,* Vol. 13, 1965, p. 1111.

Sonett, C. P.; and Colburn, D. S.: The SI^+–SI^- Pair and Interplanetary Forward-Reverse Shock Ensembles. *Planet. Space Sci.,* Vol. 13, 1965, p. 675.